J Mater Sci: Mater Electron **(2025) 36:1552**

Analysis of barrier inhomogeneity in SiC schottky diodes with P3HT: PCBM interfaces over a wide temperature range

Tamer Güzel[1,2,*]

[1] *Mechatronic Department, Vocational School of Technical Sciences, Niğde Ömer Halisdemir University, Niğde, Türkiye*
[2] *Central Research and Application Laboratory, Kırşehir Ahi Evran University, Kırşehir, Türkiye*

Received: 4 June 2025
Accepted: 20 August 2025
Published online: 29 August 2025

ABSTRACT

Research on the metal–semiconductor interface continues due to its significant impact on the electrical characteristics of Schottky diodes. In this study, a Schottky diode with the structure Au/P3HT: PCBM/6H–SiC/Al was fabricated, and its current–voltage characteristics were analyzed over a wide temperature range of 80–375 K. Using these characteristics, the ideality factor (n), barrier height (Φ_b), resistance (Rs), and saturation current (I_o) parameters of the diode were calculated with the help of the Thermionic emission model, Cheung-Cheung, and Norde functions. The correlation between these parameters was also examined. The Richardson constant (A^*) was determined using the Richardson plot. Furthermore, the barrier inhomogeneity was analyzed based on a Gaussian distribution model. Although the barrier height has an inhomogeneity showing a double Gaussian distribution that varies with temperature, the effect of voltage deformation was determined to be stable at all temperatures.

1 Introduction

A different dimension has been achieved in controlling electrons with a special barrier formed at the interface in the case of metal–semiconductor contacts and resulting from the difference in the conductivity mechanism of the contact materials. Thanks to these developments, electronic components have formed the basis of electronics science and industry and have enabled the rapid development of these fields [1–3]. Among these electronic components, rectifier diodes are the foremost elements. Despite the widespread use of these diodes, their working methods are still not clearly understood, and the formation dynamics and conduction mechanism of the electrical current formed on these contacts and its effect on the electrical barrier are still the subject of research. The thermionic emission model, which is used especially in the examination of these diodes, is accepted as the basis, and in recent years, artificial intelligence has also been included in research on this subject [4–6]. In this theory, the current conduction mechanism of a diode, excluding constants and environmental parameters, is defined by four basic concepts. These are barrier height, ideality factor, resistance, and saturation current. One of the best tools for determining these

Address correspondence to E-mail: tamerguzel7840@gmail.com

https://doi.org/10.1007/s10854-025-15643-9

parameters is the determination of current–voltage characteristics depending on temperature. Because, apart from the calculation of some constants, the main reason why diodes are determined depending on temperature is that these diodes are used in a very wide temperature range. However, these parameters are insufficient to explain the behavior of diodes, especially at low temperatures. In particular, a complete understanding of the current conduction mechanism occurring on diodes is the key factor in both optimizing diodes produced with complex processes and producing more stable and industrially acceptable quality products. Among the factors that significantly affect the fundamental parameters of diodes, the polymers used at the interface are of particular importance [7]. One of these materials is conductive polymers consisting of a mixture of Poly(3-hexylthiophene) (P3HT) as an electron donor and [6, 6]-Phenyl-C_{61}-butyric acid methyl ester (PCBM) as an electron acceptor. Due to its ease of application and low cost, it is used today for many applications and research on diodes [8]. In addition, this polymer mixture is among the indispensable components in organic solar cell applications [9, 10]. Particularly, due to the structurally conductive nature of this polymer, Schottky diodes attract considerable attention in terms of interfacial engineering. Although there are very few and limited studies in the literature on the use of P3HT: PCBM polymer interface layer especially in silicon carbide-based diodes, there are a few studies on the applications of this polymer on different semiconductor-based diodes. Altan et al. determined the electrical parameters of a 6H-SiC based Schottky diode with a P3HT: PCBM polymer interface in the temperature range of 300–375 K. They reported that this polymer affects the density of interface states and current–current conduction [11]. Özmen investigated the effect of different volumetric ratios of P3HT: PCBM conductive polymer formed at the interface during the production of a silicon-based diode on the electrical parameters of the diode at room temperature. He showed that increasing the PCBM ratio in the polymer layer in the mixed state improved the diode quality [12]. Yağlıoğlu et al. investigated the effect of F4-TCNQ (4,7-Dimethyloxy-2,3,5,6-tetrafluoroquinone) concentration on the electrical parameters of the interface layer of P3HT: PCBM polymer and silicon-based Schottky diode at room temperature. They stated that 1% F4-TCNQ doping rate to the interface layer caused an improvement in the electrical parameters of the Schottky diode [13]. Demirezen et al. investigated the electrical parameters of the silicon Schottky diode with P3HT: PCBM polymer interlayers containing different volumetric ratios of graphene oxide at room temperature in the dark and under different light intensities. They stated that the amount of graphene oxide doped into the interfacial polymer layer affects the basic parameters of the diode such as ideality factor, barrier height, resistance, and interfacial density of states [14].

In this study, Schottky diode with a polymer interface having the Au/P3HT: PCBM/n-6H–SiC/Al structure was fabricated and the current–voltage characteristics of this diode were determined in a wide temperature range (80–375 K) for the first time in the literature. Using these temperature-dependent characterization sets, basic electrical parameters such as ideality factor, Schottky barrier height, series resistance, saturation current, and Richardson constant were calculated with various methods; the obtained results were evaluated comparatively both with the studies in the literature and in terms of correlation between the methods. Additionally, the inhomogeneity analysis in the barrier height was performed on the obtained temperature-dependent current–voltage characteristic, and the results were reported.

2 Experimental section

In the fabrication of the Schottky diode, a 2-inch diameter (0 0 1) oriented 280 μm thick n-type 6H-SiC semiconductor wafer with a donor density of 2.6×10^{17} cm^{-3} was used as the base material. The semiconductor wafer used was cleaned in an ultrasonic bath for 5 min with trichloroethylene, acetone, and methanol, respectively, and then rinsed with deionized water. After the rinsing process was completed, the sample was kept in $HF + H_2O$ (1:20) solution for 15 s to prevent the formation of an oxide layer on the surface. Pure Au (99.995%) with a thickness of 150 nm was evaporated onto the matte surface of the semiconductor under 10^{-6} Torr pressure and the sample was annealed at 950 °C for 5 min in the metal evaporation system to create ohmic contact. To coat the poly(3-hexylthiophene) (P3HT): [6,6]-Phenyl-C_{61}-butyric acid methyl ester (PCBM) layer, a P3HT: PCBM solution prepared by dissolving the components in dichlorobenzene at 60 °C in a 1:1 volume ratio was dropped (three drops) onto the sample placed in the device, and the spin-coating apparatus was then operated. The spin-coating process was performed at

1000 rpm/s for 2 min to obtain a uniform thin film. After the process was completed, the sample was placed in a heating oven at 80 °C for about 10 min to allow the dichlorobenzene in the solution to evaporate and separate from the sample.

After this process, a P3HT: PCBM (1:1) layer of approximately 120 nm was formed on the shiny surface of 6H-SiC, as determined by profilometer. In order to create a rectifying contact, approximately 150 nm thick pure aluminum (Al) (99.999%) was evaporated. In these processes, a stainless steel mask was used to create 1 mm diameter contacts. For current–voltage (I–V) measurements, Keithley 2400 Sourcemeter was used. The measurements were performed by controlling an IEEE-488 AC/DC converter card connected to the computer. The measurements were made in the voltage range of − 2 V to + 3 V with 0.02 V increments and in the temperature scale of 80–375 K. The Au/P3HT: PCBM (1:1)/6H-SiC/Al Schottky diode that was fabricated is shown in Fig. 1.

3 Results and discussion

Electrical characterization methods rely on measurement techniques described in standard literature to accurately determine the parameters of semiconductors. Among these, current–voltage (I–V) measurements can be used to determine parameters such as conduction mechanisms, Schottky barrier height, ideality factor, and series resistance [15]. These parameters can be obtained using the thermionic emission model. According to this model, the relationship between current and voltage is expressed as in Eqs. 1 and 2.

$$I = I_o \exp\left(\frac{qV}{nkT}\right)\left[1 - \exp\left(\frac{-qV}{kT}\right)\right] \quad (1)$$

$$I_0 = AA^{**}\exp\left(\frac{-q\Phi_b}{kT}\right) \quad (2)$$

Here I_o is the saturation current, V is the applied voltage, q is the electron charge, T is the absolute temperature, A is the contact area, k is the Boltzmann constant, Φ_b is the Schottky barrier height, n is the ideality factor, and A^* is the Richardson coefficient of the semiconductor. For the n-6H-SiC used here, this coefficient is equal to 146 Acm^{-2} K^{-2} [16]. The terms for the ideality factor (n) and the barrier height (Φ_b) from Eq. 1 and 2 are expressed in Eqs. 3 and 4, respectively.

$$n = \frac{q}{kT}\left(\frac{dV}{dlnI}\right) \quad (3)$$

$$\Phi_b = \frac{kT}{q}\,\mathrm{Ln}\left(\frac{AA * T^2}{I_0}\right) \quad (4)$$

Using the LnI-V plot obtained from experimental current–voltage measurements, Eq. 3 and 4, the most important electrical parameters for diodes, Φ_b, n and I_o, can be calculated, which are the most important parameters for defining the relationship between voltage and current according to the Thermionic emission theory.

Accordingly, n can be calculated from the slope of the linear region of the LnI-V plot using Eq. 3, and I_o can be determined from the cut-off point. In addition, the Φ_b value is calculated using these values according to Eq. 4. The experimental current–voltage characteristics of the P3HT: PCBM/6H-SiC/Al diode are shown in Fig. 2 on a semi-logarithmic scale. Accordingly, the parameters calculated according to Fig. 2 using the equations are shown in Table 1. One of the important parameters among these parameters is the resistance, which affects the current conduction mechanism, especially in high-voltage sections. Many methods, including artificial intelligence, have been proposed in the literature to determine the resistances [5].

Among these methods, two methods stand out. The first is the Cheung-Cheung method and the other is the Norde method [17, 18]. In the Cheung-Cheung method, according to Eq. 5, the plot of the dV/dLnI ratio versus

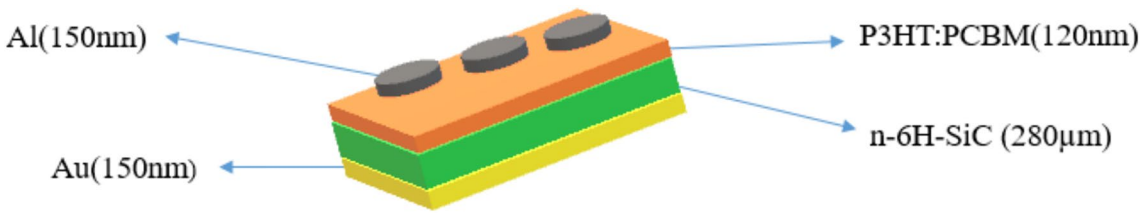

Fig. 1. Schematic illustration of the Au/P3HT: PCBM/6H–SiC/Al Schottky diode structure

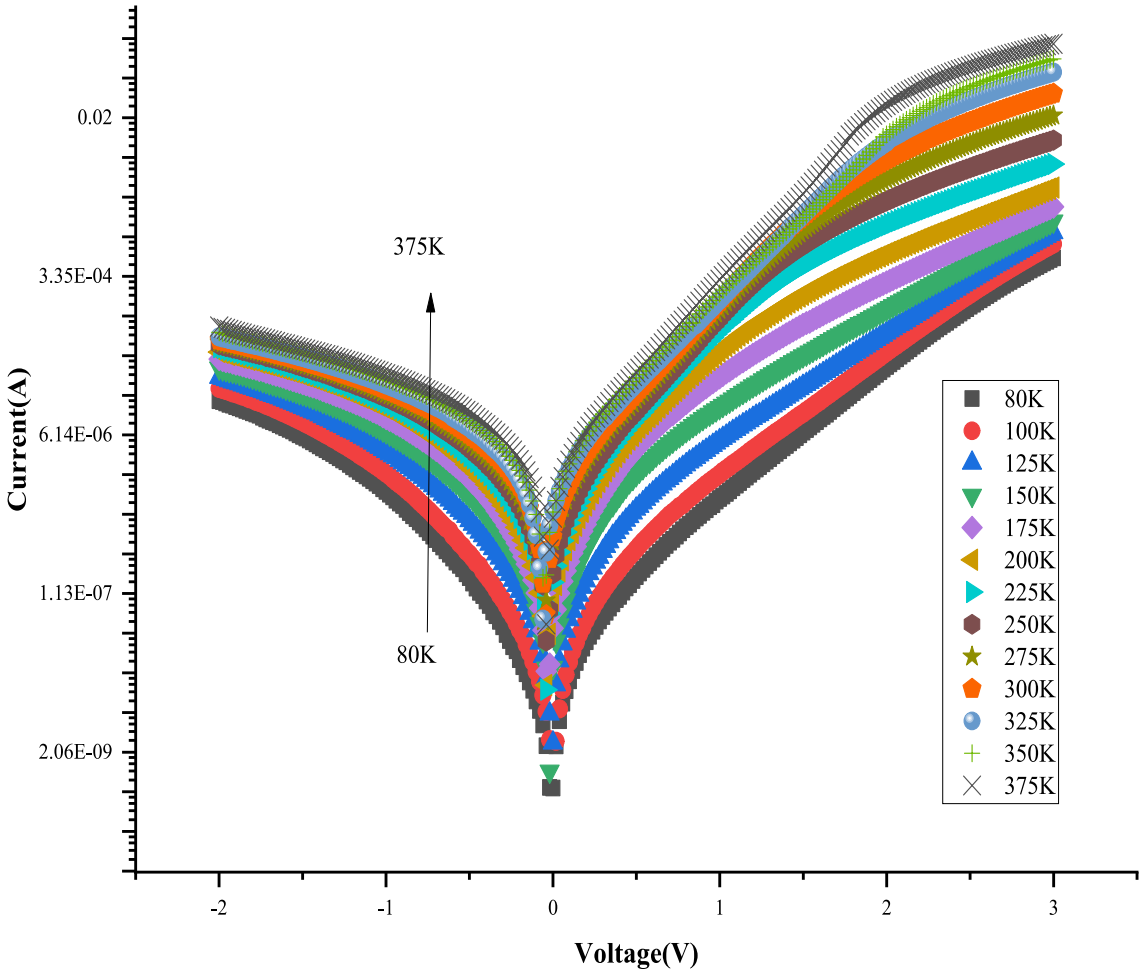

Fig. 2. Semi-logarithmic current–voltage (I–V) characteristics of the Au/P3HT/6H–SiC/Al Schottky diode measured in the temperature range of 80–375 K

Table 1. Determined electrical parameters of P3HT: PCBM/6H-SiC/Al diode

T(K)	Φ_b(eV) I–V	Φ_b(eV) F(V)–V	Φ_b(eV) H(I)–I	n I–V	n dV/dLn(I)-I	Rs(kΩ) H(I)–I	Rs(kΩ) F(V)–V	Rs(kΩ) dV/dLn(I)	Io(A)
80	0.19	0.19	0.19	18.87	15.61	848.08	507.50	1475.05	6.88×10^{-9}
100	0.24	0.23	0.24	12.86	11.42	418.38	343.05	709.35	9.00×10^{-9}
125	0.29	0.26	0.29	10.52	9.28	152.05	107.48	235.02	2.58×10^{-8}
150	0.34	0.34	0.34	8.62	7.21	61.17	27.78	112.21	5.51×10^{-8}
175	0.39	0.39	0.39	7.28	6.51	30.33	30.16	54.10	1.03×10^{-7}
200	0.45	0.44	0.45	6.72	6.14	18.03	13.53	30.60	1.82×10^{-7}
225	0.50	0.49	0.50	6.15	5.43	14.00	14.70	24.90	2.92×10^{-7}
250	0.55	0.54	0.55	5.63	4.60	13.47	12.76	24.83	3.90×10^{-7}
275	0.60	0.59	0.60	5.41	4.67	10.24	9.41	17.14	6.50×10^{-7}
300	0.65	0.64	0.65	5.26	4.11	9.38	7.33	16.52	8.55×10^{-7}
325	0.70	0.69	0.70	5.02	3.84	7.62	6.70	15.55	1.28×10^{-6}
350	0.75	0.74	0.75	4.87	3.60	6.38	6.17	12.83	1.52×10^{-6}
375	0.80	0.79	0.81	4.42	3.35	5.25	5.39	10.93	9.98×10^{-6}

the current (I) should yield a straight line. Rs is calculated from the slope of this line, and the n value is determined from the vertical axis intercept point. However, the $H(I)$ function is defined as given in Eq. (6). A yield a straight line is also expected from the plot of the $H(I)$ function versus current. According to Eq. (7), the slope of this line gives the Rs value, while the intercept on the vertical axis yields the barrier height (Φ_b). The calculated parameters n. Φ_b and Rs calculated according to the Cheung-Cheung method are shown in Table 1.

$$\frac{dV}{dLnI} = IR_s + \frac{nkT}{q} \tag{5}$$

$$H(I) = V - n(\frac{kT}{q})\ln(\frac{I}{AA^*T^2}) \tag{6}$$

$$H(I) = IR_s + n\Phi_b \tag{7}$$

In addition, the plots obtained depending on the temperature according to the Cheung-Cheung method, the plots obtained at room temperature, and the line fitted for 300 K are shown in Figs. 3 and 4. In the other method, Norde, a function is defined as in Eq. 8.

$$F(V) = \frac{V}{\gamma} - \frac{1}{\beta}\ln\left(\frac{I(V)}{AA^{**}T^2}\right) \tag{8}$$

Here, if $\beta = q/kT$ and γ is a number greater than ideality (n), the $F(V)$-V plot is expected to pass through a minimum. The barrier height is calculated according to Eq. 9, with V_{min} being the value corresponding to $F(V)_{min}$. The Rs value is calculated according to Eq. 10 using the current (I_{min}) value corresponding to the V_{min} value. The Φ_b and Rs parameters calculated according to the Norde function according to Eqs. 9 and 10 equations are shown in Table 1. On the other hand, the $F(V)$-V plot also obtained depending on the temperature is shown in Fig. 5.

$$\varphi_b = F_{min} + \frac{V_{min}}{\gamma} - \frac{kT}{q} \tag{9}$$

$$R_s = \frac{kT(\gamma - n)}{qI_{min}} \tag{10}$$

The calculated parameters using the current–voltage characteristics of the P3HT: PCBM/6H-SiC/Al diode in the temperature range of 80–375 K are shown in Table 1. According to the table, the ideality factor (n) was calculated as 18.87 and 5.26 for 80 K and 300 K, respectively.

The barrier height (Φ_b) was found to be 0.19 and 0.65 eV for the same temperatures, respectively. The resistance values were determined as 848kΩ and 9.38kΩ for 80 K and 300 K, respectively. In addition, the saturation current (I_o), which is one of the important characteristics of the diode, was calculated to be 6.88×10^{-9}A and 8.55×10^{-7}A at the same temperatures, respectively. The calculated parameters are also

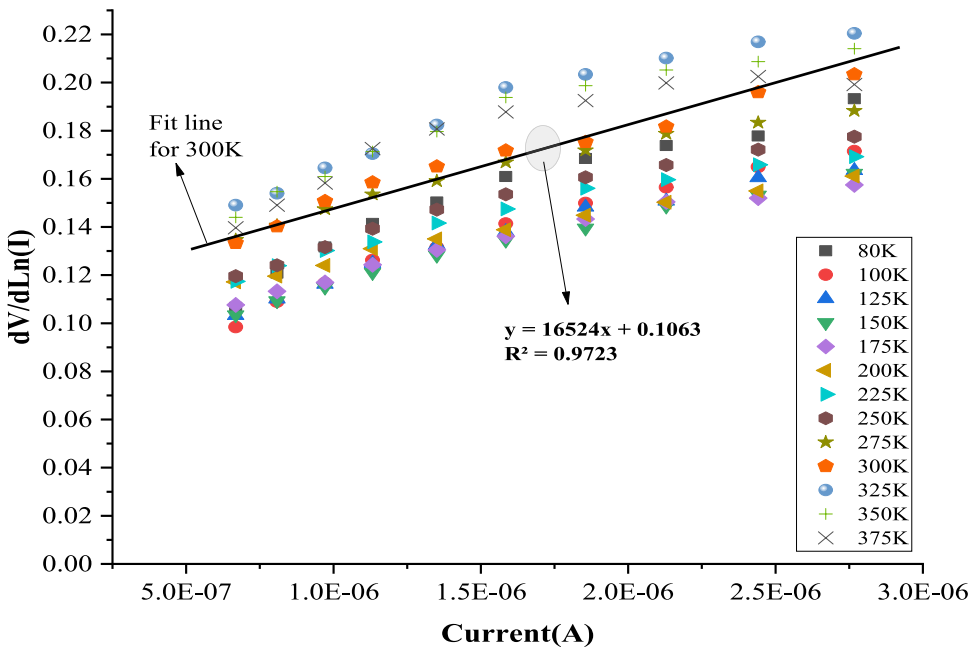

Fig. 3. dV/dLn(I)-I plot of P3HT: PCBM/6H-SiC/Al Schottky diode in the temperature range

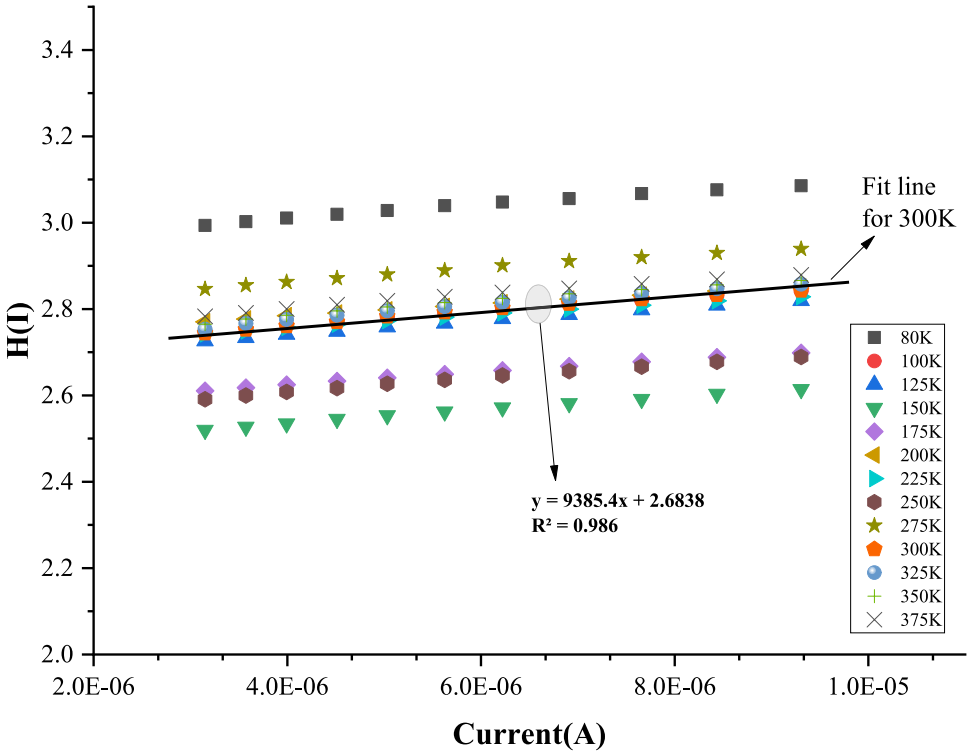

Fig. 4. *H*(I)-I plot of P3HT: PCBM/6H-SiC/Al Schottky diode in the temperature range.

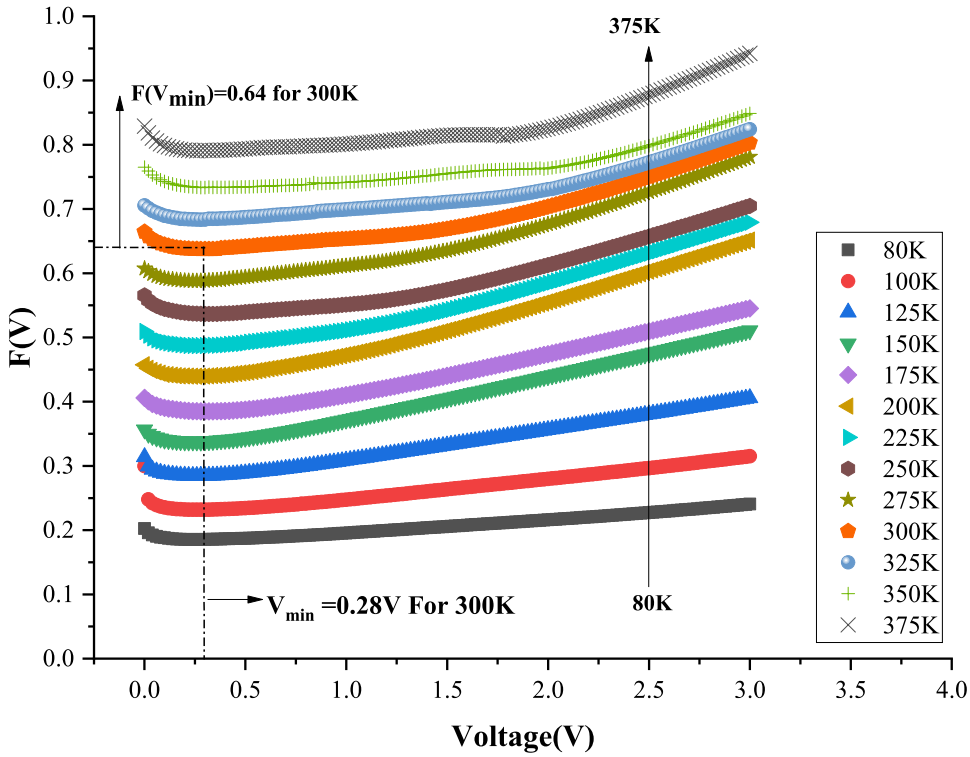

Fig. 5. *F*(*V*)-*V* plot of P3HT: PCBM/6H-SiC/Al Schottky diode in the temperature range

compatible with the literature [11]. At this point, while the n and Rs parameters decrease with the increase in temperature, the I_o and Φ_b values increase with rising temperature. One of the basic assumptions of the thermionic emission conduction mechanism is that the energy required for the carriers to form the current is provided by thermal energy. Therefore, the strong dependence of all parameters on temperature was confirmed in this study [19]. The reason for the increase in the n value and the decrease in the barrier height due to lowering the temperature could be suggested as physical reasons such as interface states and trap density, as well as the change of dominant conduction mechanisms depending on the temperature. Another reason proposed for this behavior is the non-homogeneous nature of the barrier height [20].

In fact, in the Thermionic emission model, the barrier height is assumed to be a constant value, independent of the applied voltage. This fixed barrier approach may actually be the reason why the experimentally obtained parameters differ from those expected. Because at low temperatures, the current consists of carriers that overcome a low barrier. Since this current is formed due to a barrier below the barrier height predicted by the thermionic emission model, the n value is calculated very differently at these temperatures. As the temperature increases, more carriers overcome the barrier from certain patches, and in this case, while Φ_b approaches the value predicted by the theory, the dominant current mechanism evolves into the classical Thermionic model and n enters a decreasing trend. On the other hand, it can be seen that the resistance value decreases due to the increase in the number of carriers that overcome the barrier as the temperature increases. In addition, the polymer layer at the interface may have affected the electrical parameters because it causes fluctuations in the interface electrical potential. Because it has been reported in the literature that the polymer structures at the interface form volumetrically inhomogeneous interface structures due to the non-periodic and locally variable bond structure distribution, the ideality value may be much larger than expected [21]. On the other hand, the n and Φ_b parameters calculated for the diode are in good agreement with each other. However, it can be seen in Table 1 that the resistance values are calculated using the Cheung-Cheung method, although they show a good correlation with each other and differ slightly from the values calculated with the Norde method, particularly in the low-temperature region. This may arise from the different calculation approaches of the two methods. While the resistance is determined by the Cheung-Cheung method from a specific linear part in the forward bias, in the Norde method, the resistance is calculated from the entire forward bias region [22]. Another important parameter of the thermionic emission mechanism is the constant known as the Richardson constant, which indicates the semiconductor. It could be said that this constant indicates a kind of conductivity of the semiconductor depending on the temperature. This parameter can be calculated by a method known as the traditional Richardson curve. Accordingly, Eq. 11 is used to construct this curve.

$$\ln\left(\frac{I_0}{T^2}\right) = \ln\left(AA^{**}\right) - \frac{q\Phi_{b0}}{kT} \tag{11}$$

According to Eq. 11, it is expected that the Ln(I_o/T^2)-1000/T plot should yield a straight line. The slope of this plot gives the effective barrier height (Φ_{b0}) and the Richardson constant (A^*) is found from the point where it intersects the vertical axis. The Ln(I_o/T^2)-1000/T plot obtained as a result of the experimental data of the diode is shown in Fig. 6. As a result of the calculations from the plot, the values of A^* and Φ_{b0} were found to be 4.31×10^{-9} Acm^{-2} K^{-2} and 0.291 eV. When this result is examined, it is clearly seen that the known Richardson constant (A*) of 6H-SiC is much smaller than the value of 146 Acm^{-2} K^{-2}. In fact, this result has also been reported by other researchers who performed similar studies on Schottky diodes with different polymer interfaces [11, 23, 24]. Such a significant deviation in the Richardson constant may indicate that the barrier height is not homogeneous, suggesting a patchy barrier structure and potential fluctuations at the interface where low or high barrier regions are formed. Because in such a case, the current will prefer a lower barrier in an inhomogeneous barrier structure, the Richardson value (A*) calculated from the experimental current–voltage characteristics depending on the temperature may be affected by the spatial inhomogeneity of the barrier. This may lead to a calculation of the A* value quite different from the theoretical value [25, 26].

In addition, the P3HT: PCBM polymer at the interface may have affected the potential at the interface due to its spontaneous electrical dipole. Because Aarniyo et al. showed that the P3HT:PCBM polymer can naturally form an electrical dipole [27]. On the other hand, localized and irregular chemical bonds

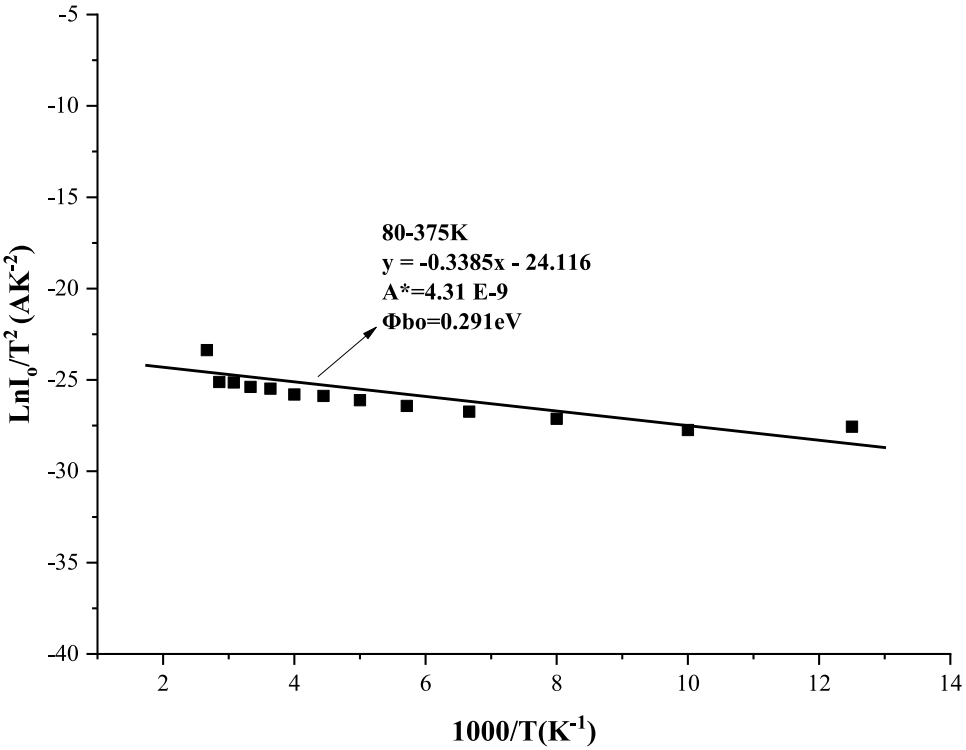

Fig. 6. Plot of LnI_o/T^2 versus 1000/T for the P3HT: PCBM/6H-SiC/Al Schottky diode

between the polymer and semiconductor could create trap levels. Furthermore, because the thermal expansion coefficients of the polymer layer and the semiconductor differ, microcracks or defect regions could contribute to these trap centers due to temperature changes. In this case, the Richardson constant may be affected, as it can affect current conduction. Horvath explained that the reason for the significant deviation of the Richardson constant could also be due to the lateral inhomogeneity of the barrier height [28]. To investigate lateral inhomogeneity, Schmitsdorf et al. proposed an approach based on Tung's theoretical model [25, 29]. They stated that a linear relationship between the barrier height and the ideality factor could be an indicator of lateral inhomogeneity. Accordingly, the variation of barrier height with respect to the ideality factor is shown in Fig. 7. As can be seen from the plot, two distinct linear regions are observed. From these regions, the mean barrier heights corresponding to the ideal case ($n = 1$) were determined. The mean barrier height was found to be 0.386 eV in the 80–150 K range, and 1.281 eV in the 175–400 K range. Based on these results, the presence of two different linear regions in Fig. 7 may indicate that the barrier is laterally inhomogeneous at different temperature intervals.

At this point, for spatial inhomogeneity, a Gaussian distribution (GD) model of the barrier height based on the thermionic emission mechanism was proposed. According to this model, the barrier height actually exhibits a distribution, which can be expressed as a Gaussian distribution $P(\Phi_{bo})$, defined as a function of the mean barrier height ($\overline{\Phi}_{bo}$) and the standard deviation (σ_0) as given in Eq. (12) [20, 30].

$$P(\Phi_{bo}) = \frac{1}{\sigma_0\sqrt{2\pi}} exp\left[-\frac{(\Phi_{b0} - \overline{\Phi}_{bo})^2}{2\sigma_0}\right] \quad (12)$$

According to this, the barrier height (Φ_b) and ideality factor (n) obtained through the application of the Gaussian distribution function to the thermionic emission model are represented as Φ_{ap} and n_{ap}, respectively. In this model, the value of Φ_{ap} is given by the equation in Eq. (13), where Φ_{ap} is the experimentally measured barrier height, σ_0 is the standard deviation, and $\overline{\Phi}_{bo}$ is the mean barrier height. Since the temperature dependence of the standard deviation σ_0 is generally small, it can be neglected in barrier height calculations. In that case, the previously described thermionic emission mechanism becomes dominant again, and the barrier height is assumed to be constant and single-valued. On the other hand, according to the GD model, the temperature dependence of the ideality factor is expressed by Eq. (14).

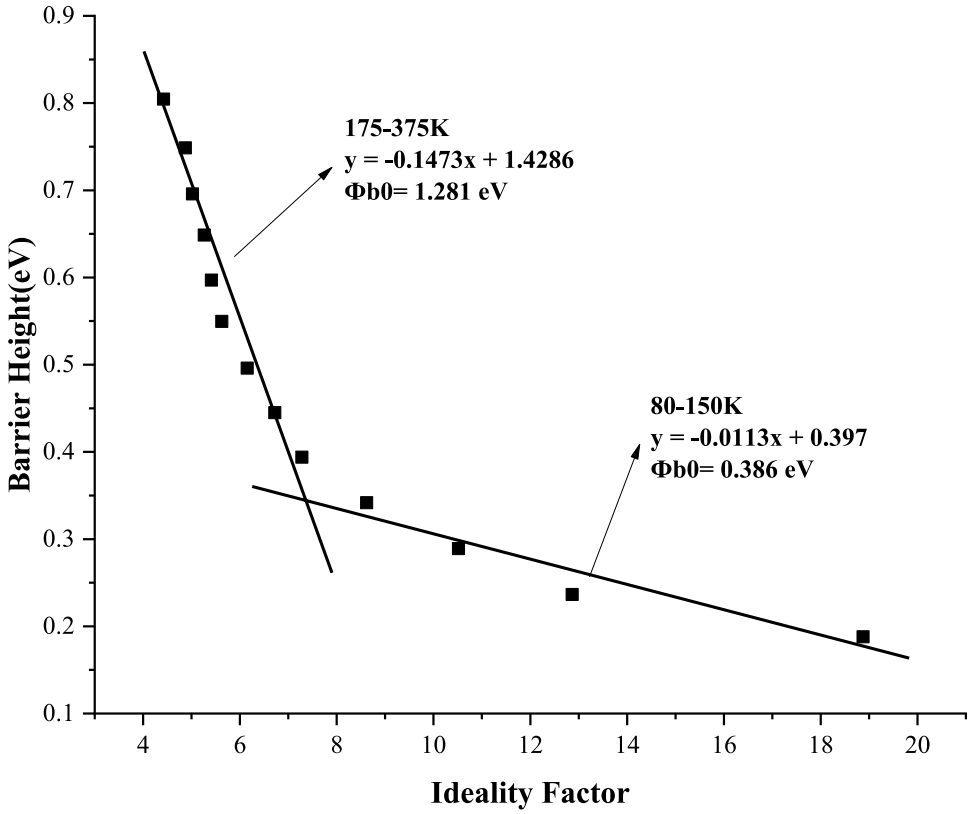

Fig. 7. Plot of barrier height versus ideality factor for the P3HT: PCBM/6H-SiC/Al diode

$$\Phi_{ap} = \overline{\Phi}_{bo}(T=0) - \frac{q\sigma_0^2}{2kT} \tag{13}$$

$$\left(\frac{1}{n_{ap}} - 1\right) = -\rho_2 + \frac{q\rho_3}{2kT} \tag{14}$$

Here n_{ap} is the experimentally calculated ideality factor, ρ_2 and ρ_3 are the voltage coefficients depending on the distribution of the barrier height. There is a linear relationship between the voltage coefficients, the mean barrier height, and the standard deviation. This can be seen in Eqs. 15 and 16.

$$\overline{\Phi}_b = \overline{\Phi}_{bo} + \rho_2 V \tag{15}$$

$$\sigma_0 = \sigma_{so} + \rho_3 V \tag{16}$$

According to Eqs. (15) and (16), unlike the pure thermionic emission model, which assumes a constant barrier height for each temperature, it can be observed that the barrier height also involves deformation depending on the applied bias. Moreover, the closer the standard deviation approaches zero, the more the barrier height tends toward homogeneity, indicating a behavior closer to the ideal thermionic emission model. For the analysis of barrier inhomogeneity based on the experimental current–voltage data of the diode, Eqs. (13) and (14) were used. According to these equations, the plot of Φ_{ap} versus q/2kT is expected to yield a straight line. From the slope of this line, the standard deviation (σ_0) is determined, and from its intercept on the vertical axis, the mean barrier height ($\overline{\Phi}_{bo}$) is obtained. Similarly, the plot of (n_{ap}^{-1}-1) versus $q/2kT$ is also expected to produce a straight line. From the slope of this line, ρ_3 is calculated, while ρ_2 is determined from the intercept on the vertical axis. The plots drawn according to Eqs. (13) and (14) are presented in Figs. 8 and 9. As seen in Fig. 8, the plot consists of two distinct linear regions. In the temperature range of 80–150 K, the parameters $\overline{\Phi}_{bo}$ and σ_0 were calculated to be 0.5 eV and 0.067 eV, respectively. Similarly, in the temperature range of 175–375 K, the same parameters were found to be 1.10 eV and 0.150 eV, respectively. These results could be evaluated as a result of the spatial inhomogeneity of the barrier due to the different barrier heights in different temperature regions. Because, since the interface structure requires

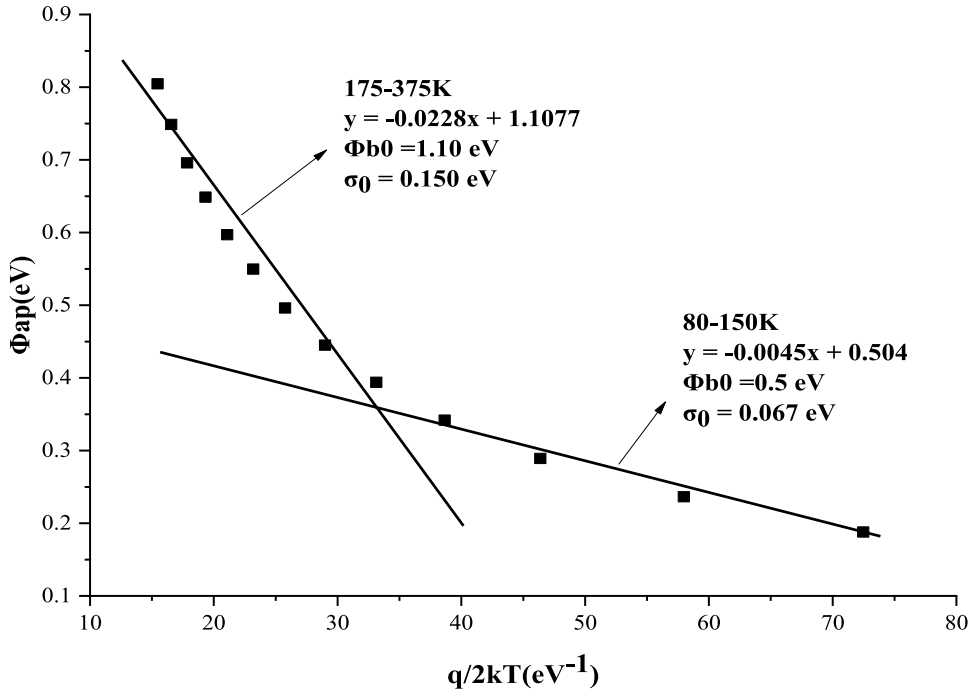

Fig. 8. Plot of Φap versus $q/2kT$ for the P3HT: PCBM/6H-SiC/Al Schottky diode with two different linear regions

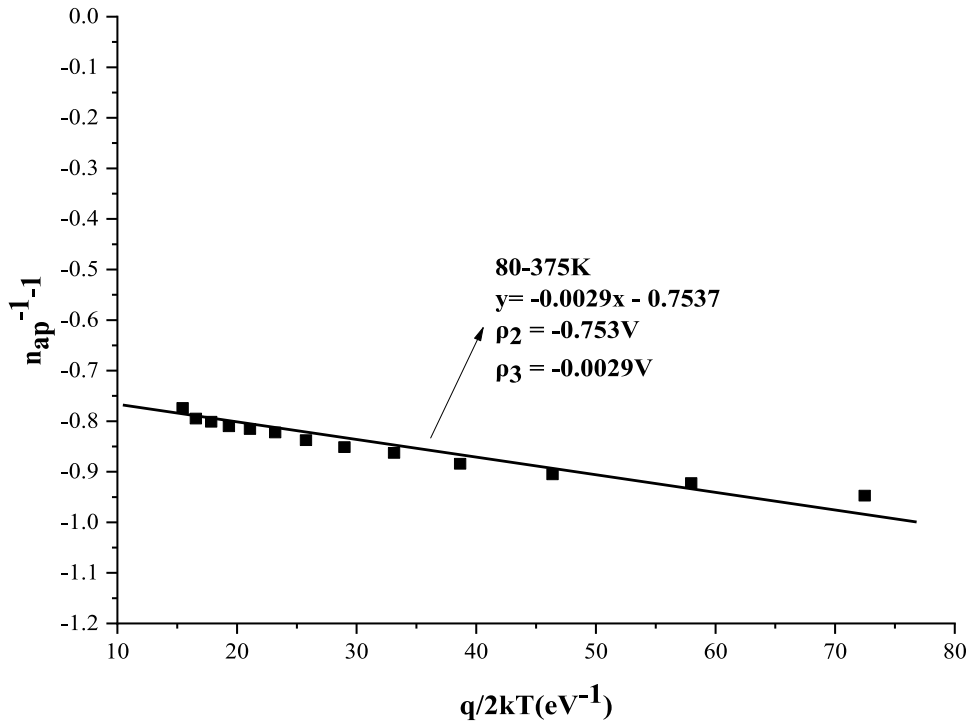

Fig. 9. Plot of n_{ap}^{-1}-1 versus q/2kT for the P3HT: PCBM/6H-SiC/Al Schottky diode with single linear region

physical contact, the electronic structure of the interface can probably be affected by dislocations, grain boundary structure, multiphases, and atomic structure of the interface as a function of the atomic lattice [26]. In addition, at high temperatures, the σ0 value corresponds to 13.63% of the calculated value of $\overline{\Phi}_{bo}$, while at low temperatures, this ratio is 13.40%. These results show that barrier inhomogeneity is relatively

effective at all temperatures and its proportional effect increases slightly as the temperature increases. In fact, the limited decrease in the ideality factor in Table 1 due to the temperature increase may be due to this reason. Furthermore, these two linear-region behaviors indicate the presence of a double Gaussian distribution of the barrier height. This phenomenon has also been reported by other researchers who previously studied silicon carbide semiconductors [31, 32].

According to the plot, the voltage coefficients ρ_2 and ρ_3 were determined as -0.75 V and -0.029 V, respectively. The negative value of both voltage constants indicates that the barrier height increases with the rise in the applied voltage of the diode, in the opposite direction of the effect of the image force lowering of the barrier [33]. Indeed, similar results have been reported in the literature [16, 34, 35]. The noticeable situation here is that while the mean barrier height exhibits two linear regions in Fig. 8, a single linear region is seen in Fig. 9. This situation is quite rare according to the literature. This observation reveals that, in terms of its effect on the barrier height, the applied voltage exhibits an effectively homogeneous influence across the entire temperature range. This situation indicates the existence of a barrier structure that is inhomogeneous in temperature sensitivity but stable to the deformation effects of voltage. In this respect, it shows that the voltage-dependent effects of the barrier patches are limited, unlike the temperature. At this point, it should be noted that in a previously reported study by Güzel et al., the aforementioned mean barrier height and voltage coefficient plots of the 6H-SiC/Au diode produced without a polymer interface, unlike this study, exhibited a two-region structure, which is well known according to the literature [32].

Moreover, with the inclusion of the calculated standard deviations, the Richardson equation can be modified as shown in Eq. (17).

$$\ln\left(\frac{I_0}{T^2}\right) - \left(\frac{q^2\sigma^2}{2k^2T^2}\right) = \ln(AA*) - \frac{q\overline{\Phi}_{b0}}{kT} \tag{17}$$

Accordingly, the $\mathrm{Ln}(I_0/T^2)$-$q^2{\sigma_0}^2/2\mathrm{k}^2T^2$ according to $1000/T$ obtained by using Eq. 17 by including the standard deviation values (σ_0) previously calculated from the linear sections for the diode is shown in Fig. 10. Accordingly, the plot of $\mathrm{Ln}(I_0/T^2)$-$q^2{\sigma_0}^2/2k^2\mathrm{T}^2$ according to $1000/T$ should yield a straight line. The mean barrier height ($\overline{\Phi}_b$) was found from the slope of this line and the Richardson constant (A*) was found

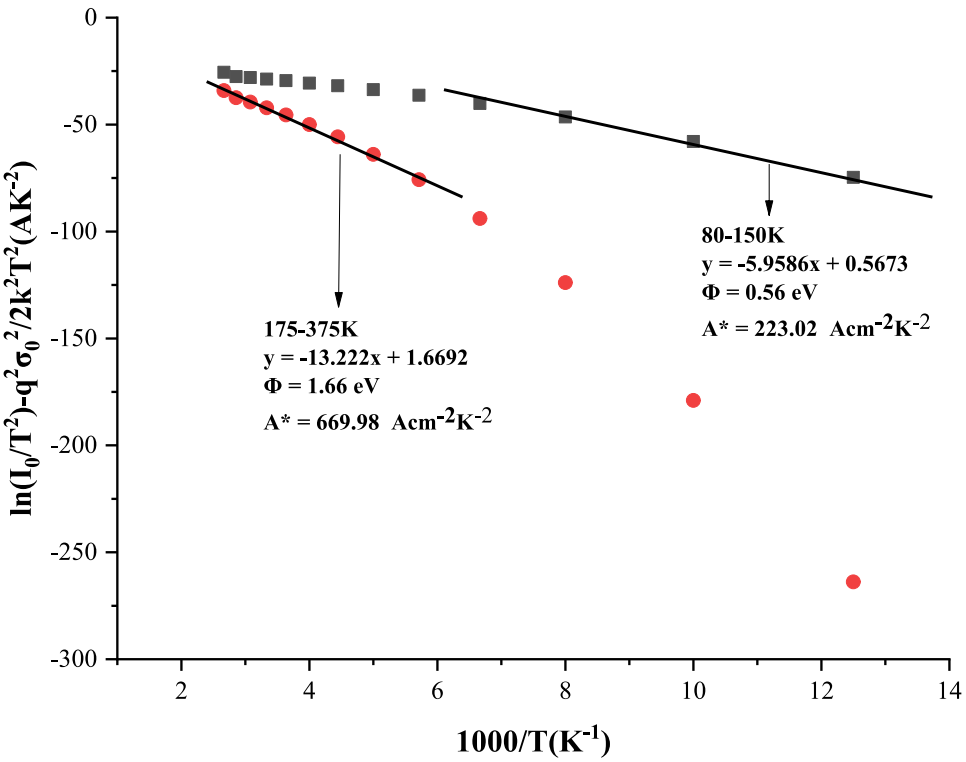

Fig. 10. Plot of $\mathrm{Ln}(I_0/T^2)$-$q^2\sigma_0^2/2k^2T^2$ versus $1000/T$ for the P3HT:PCBM/6H-SiC/Al Schottky diode

from the vertical axis cut point. According to Fig. 10, the plot prepared according to two different standard deviation values for the diode can be seen. In the temperature range of 80 K to 150 K, the mean barrier height and Richardson constant were calculated as 0.56 eV and 223.02 $Acm^{-2} K^{-2}$, respectively. On the other hand, the mean barrier height and Richardson constant calculated from the curve drawn for 175 K to 375 K were found to be 1.66 eV and 669.98 $Acm^{-2} K^{-2}$, respectively. The calculated A* values are in compatible with the known values for 6H-SiC in terms of magnitude compared to the previously calculated values. In addition, the calculated mean barrier height in the high-temperature regions is also quite good point compared to previous experimental reports of 6H-SiC/Al contacts [11, 36]. At this point, the fact that the values calculated from the modified Richardson plot accounting for standard deviation exhibit better agreement with the known theoretical value for 6H–SiC suggests that the barrier is not spatially homogeneous and exhibits inhomogeneity based on a Gaussian distribution function. On the other hand, it is necessary to state that although the mean barrier height value calculated with the effect of the P3HT: PCBM polymer layer is at a very good point compared to the literature, the ideality factor is also at a large value, especially in the high-temperature region. A similar result was reported by Gökçen et al. who explaned that although the polymer layer on the interface of the Schottky diode provides an improvement in the barrier height, it negatively affects the ideality factor [37].

4 Conclusion

A polymer-interfaced Au/P3HT\:PCBM/6H-SiC/Al Schottky diode was fabricated, and its current–voltage characteristics were determined in the temperature range of 80–375 K. At 80 K and 375 K, the ideality factors and barrier heights were calculated as 16.87 and 0.19 eV, and 4.42 and 0.80 eV, respectively. The saturation currents at the same temperatures were found to be 6.88×10^{-9} A and 9.98×10^{-6} A, respectively. The resistance values were also determined as 848 kΩ and 5.25 kΩ at the same temperatures. Based on these results, it was observed that the barrier height and saturation current increased with rising temperature, while the ideality factor and resistance decreased. Accordingly, a strong temperature dependence of the electrical parameters was confirmed. In addition, the basic parameters were calculated using the Cheung-Cheung and Norde functions. The calculated parameters showed a good correlation with each other. In addition, the inhomogeneity analysis of the barrier was performed. As a result of the analysis, two different regional distributions were determined. In the low-temperature region (80-150 K), the mean barrier height and standard deviation were calculated as 0.5 eV and 0.067, while in the high-temperature region (175-375 K) they were found to be 1.10 eV and 0.15, respectively. This is show taht at high temperatures, the σ0 value corresponds to 13.63% of the calculated value of $\overline{\Phi}_{b_0}$, while at low temperatures this ratio is 13.40%. These results demonstrated that the effect of barrier inhomogeneity relatively increased with rising temperature. Moreover, from the modified Richardson plot, the Richardson constants were found to be 223.02 and 669.98$Acm^{-2} K^{-2}$ for the low- and high-temperature regions, respectively. Similarly, the mean barrier heights in the same-temperature regions were determined to be 0.56 eV and 1.66 eV, respectively. These results showed that the barrier structure of the polymer interface diode included spatial inhomogeneity. Also, the voltage coefficients ρ_2 and ρ_3 were calculated as -0.75 V and -0.029 V, respectively. In addition, according to the lateral inhomogeneity research of the barrier height, it was determined that the barrier also contained lateral inhomogeneity.

When these results are evaluated together, it was determined that the barrier height exhibits a temperature-sensitive inhomogeneous structure, yet remains stable against voltage-induced deformation effects. This indicates that the voltage-dependent effects of the barrier patches are limited, unlike the influence of temperature. At this point, the results of this study are in good agreement with the scenario in which the barrier height is also influenced by the interfacial polymer, following a structure known as a double Gaussian distribution and consisting of spatial patches.

Funding

The authors have not disclosed any funding.

Data availability

The data are available from the corresponding author on reasonable request.

Declarations

Conflict of interest The author declares that I have no known competing financial interests or personal relationships that could have appeared to influence the work reported in this paper.

References

1. B. Sharma, *Metal-semiconductor Schottky Barrier Junctions and Their Applications* (Springer, Berlin, 2013)
2. M. Bhatnagar, B.J. Baliga, Comparison of 6H-SiC, 3C-SiC, and Si for power devices. IEEE Trans. Electron Devices **40**, 645–655 (2002)
3. F. La Via, D. Alquier, F. Giannazzo, T. Kimoto, P. Neudeck, H. Ou, A. Roncaglia, S.E. Saddow, S. Tudisco, Emerging SiC applications beyond power electronic devices. Micromachines. **14**, 1200 (2023)
4. P. Wangyang, X. Huang, X.-L. Shi, N. Zhang, Y. Ye, S. Zhao, J. Zhang, Y. Liu, F. Zhang, X. Liu, Advances in Schottky parameter extraction and applications. J. Mater. Sci. Technol. (2024)
5. O.Y. Olikh, Review and test of methods for determination of the Schottky diode parameters. J. Appl. Phys. (2015). https://doi.org/10.1063/1.4926420
6. T. Güzel, A.B. Çolak, Investigation of the usability of machine learning algorithms in determining the specific electrical parameters of Schottky diodes. Mater. Today Commun. **33**, 104175 (2022)
7. S. Ying, Z. Ma, Z. Zhou, R. Tao, K. Yan, M. Xin, Y. Li, L. Pan, Y. Shi, Device based on polymer Schottky junctions and their applications: a review. IEEE Access. **8**, 189646–189660 (2020)
8. A.J. Heeger, Semiconducting polymers: the third generation. Chem. Soc. Rev. **39**, 2354–2371 (2010)
9. H. Li, D. He, Q. Zhou, P. Mao, J. Cao, L. Ding, J. Wang, Temperature-dependent Schottky barrier in high-performance organic solar cells. Sci. Rep. **7**, 40134 (2017)
10. T. Chargui, F. Lmai, A. Erraji, Advancements in P3HT: PCBM solar cells through experimental and simulated techniques. J. Opt. **26**, 075901 (2024)
11. H. Altan, M. Özer, H. Ezgin, Investigation of electrical parameters of Au/P3HT:PCBM/n-6H–SiC/Ag Schottky barrier diode with different current conduction models. Superlattices Microstruct. **146**, 106658 (2020)
12. Ö.T. Özmen, Effects of PCBM concentration on the electrical properties of the Au/P3HT: PCBM/n-Si (MPS) schottky barrier diodes. Microelectron. Reliab. **54**, 2766–2774 (2014)
13. E. Yağlıoğlu, Ö.T. Özmen, F4-TCNQ concentration dependence of the current—voltage characteristics in the Au/P3HT: PCBM: F4-TCNQ/n-Si (MPS) Schottky barrier diode. Chin. Phys. B **23**, 117306 (2014)
14. S. Demirezen, A. Dere, H. Çetinkaya, A. Al-Sehemi, A. Al-Ghamdi, F. Yakuphanoglu, Hybrid photonic device based on graphene oxide (GO) doped P3HT-PCBM/p-silicon for photonic applications. Phys. Scr. **98**, 115916 (2023)
15. A. Azarov, A. Hallén, H.H. Radamson, Electrical characterization of semiconductors: I-V, C–V and hall measurements, in *Analytical Methods and Instruments for Micro- and Nanomaterials*. (Springer, 2023), pp.197–240
16. A. Bekaddour, A. Rabehi, S. Tizi, B. Zebentout, B. Akkal, Z. Benamara, Effect of the contact area on the electrical characteristics of the Ti/6H–SiC (n) schottky diode. Micro. Nanostruct. **173**, 207464 (2023)
17. S. Cheung, N. Cheung, Extraction of Schottky diode parameters from forward current-voltage characteristics. Appl. Phys. Lett. **49**, 85–87 (1986)
18. H. Norde, A modified forward I-V plot for Schottky diodes with high series resistance. J. Appl. Phys. **50**, 5052–5053 (1979)
19. A. Türüt, On current-voltage and capacitance-voltage characteristics of metal-semiconductor contacts. Turk. J. Phys. **44**, 302–347 (2020)
20. J.H. Werner, H.H. Güttler, Barrier inhomogeneities at Schottky contacts. J. Appl. Phys. **69**, 1522–1533 (1991)
21. S. Sönmezoğlu, S. Şenkul, R. Taş, G. Çankaya, M. Can, Electrical characteristics of an organic thin copolymer/p-Si Schottky barrier diode. Thin Solid Films **518**, 4375–4379 (2010)
22. T. Güzel, A.B. Çolak, Performance prediction of current-voltage characteristics of Schottky diodes at low temperatures using artificial intelligence. Microelectron. Reliab. **147**, 115040 (2023)
23. J. Felix, M. Aziz, D. Da Cunha, K. Seidel, I. Hümmelgen, W. De Azevedo, E. da Silva Jr, D. Taylor, M. Henini, Investigation of deep-level defects in conductive polymer on n-type 4H-and 6H-silicon carbide substrates using IV and deep level transient spectroscopy techniques. J. Appl. Phys. **112**, 014505 (2012)
24. M.H. Al-Dharob, H.E. Lapa, A. Kökce, A.F. Özdemir, D.A. Aldemir, Ş Altındal, The investigation of current-conduction mechanisms (CCMs) in Au/(0.07 Zn-PVA)/n-4H-SiC

(MPS) Schottky diodes (SDs) by using (IVT) measurements. Mater. Sci. Semicond. Process. **85**, 98–105 (2018)
25. R. Tung, Electron transport at metal-semiconductor interfaces: general theory. Phys. Rev. B **45**, 13509 (1992)
26. J. Sullivan, R. Tung, M. Pinto, W. Graham, Electron transport of inhomogeneous Schottky barriers: a numerical study. J. Appl. Phys. **70**, 7403–7424 (1991)
27. H. Aarnio, P. Sehati, S. Braun, M. Nyman, M.P. de Jong, M. Fahlman, R. Österbacka, Spontaneous charge transfer and dipole formation at the interface between P3HT and PCBM. Adv. Energy Mater. **1**, 792–797 (2011)
28. Z.J. Horvath, Comment on "Analysis of IV measurements on $CrSi_2$- Si Schottky structures in a wide temperature range." Solid-State Electron. **39**, 176–178 (1996)
29. R. Schmitsdorf, T. Kampen, W. Mönch, Explanation of the linear correlation between barrier heights and ideality factors of real metal-semiconductor contacts by laterally nonuniform Schottky barriers. J. Vac. Sci. Technol. B Microelectron. Nanometer Struct. Process. Meas. Phenom. **15**, 1221–1226 (1997)
30. Y. Song, R. Van Meirhaeghe, W. Laflere, F. Cardon, On the difference in apparent barrier height as obtained from capacitance-voltage and current-voltage-temperature measurements on Al/p-InP Schottky barriers. Solid-State Electron. **29**, 633–638 (1986)
31. Y.-H. Wang, Y.-M. Zhang, Y.-M. Zhang, Q.-W. Song, R.-X. Jia, Al/Ti/4H-SiC Schottky barrier diodes with inhomogeneous barrier heights. Chin. Phys. B **20**, 087305 (2011)
32. T. Güzel, A.K. Bilgili, M. Özer, Investigation of inhomogeneous barrier height for Au/n-type 6H-SiC Schottky diodes in a wide temperature range. Superlattices Microstruct. **124**, 30–40 (2018)
33. N. Yıldırım, A. Türüt, A theoretical analysis together with experimental data of inhomogeneous Schottky barrier diodes. Microelectron. Eng. **86**, 2270–2274 (2009)
34. T. Zhang, C. Raynaud, D. Planson, Measure and analysis of 4H-SiC Schottky barrier height with Mo contacts. Eur. Phys. J. Appl. Phys. **85**, 10102 (2019)
35. V. Kumar, A.S. Maan, J. Akhtar, Barrier height inhomogeneities induced anomaly in thermal sensitivity of Ni/4H-SiC Schottky diode temperature sensor. J. Vac. Sci. Technol. B Nanotechnol. Microelectron. Mater. Process. Meas. Phenom. (2014). https://doi.org/10.1116/1.4884756
36. A. Syrkin, A. Andreev, A.A. Lebedev, M. Rastegaeva, V. Chelnokov, Metal–n-6H–SiC surface barrier height—experimental data and description in the traditional terms. J. Appl. Phys. **78**, 5511–5514 (1995)
37. M. Gökçen, T. Tunç, Ş Altındal, I. Uslu, The effect of PVA (Bi2O3-doped) interfacial layer and series resistance on electrical characteristics of Au/n-Si (110) Schottky barrier diodes (SBDs). Curr. Appl. Phys. **12**, 525–530 (2012)